

Magnetic flux density and the critical field in the intermediate state of type-I superconductors

V. Kozhevnikov,¹ R. J. Wijngaarden,² J. de Wit,² and C. Van Haesendonck³

¹Tulsa Community College, Tulsa, Oklahoma 74119, USA

²VU University Amsterdam, 1081 HV Amsterdam, The Netherlands

³Laboratory of Solid-State Physics and Magnetism, KU Leuven, BE-3001 Leuven, Belgium

(Received 14 March 2013; revised manuscript received 15 February 2014; published 10 March 2014)

To address unsolved fundamental problems of the intermediate state (IS), the equilibrium magnetic flux structure and the critical field in a high-purity type-I superconductor (indium film) are investigated using magneto-optical imaging with a three-dimensional vector magnet and electrical transport measurements. The least expected observation is that the critical field in the IS can be as small as nearly 40% of the thermodynamic critical field H_c . This indicates that the flux density in the *bulk* of normal domains can be *considerably* less than H_c , in apparent contradiction with the long-established paradigm, stating that the normal phase is unstable in fields below H_c . Here we present a theoretical model consistently describing this and *all* other properties of the IS. Moreover, our model, based on a rigorous thermodynamic treatment of the observed equilibrium flux structure in a tilted field, allows for a *quantitative* determination of the domain-wall parameter and the coherence length, and provides new insight into the properties of superconductors.

DOI: [10.1103/PhysRevB.89.100503](https://doi.org/10.1103/PhysRevB.89.100503)

PACS number(s): 74.78.-w, 74.25.Gz, 74.25.Ha, 74.25.Op

The interest in domain shapes and patterns in a big variety of physicochemical systems with spatially modulated phases [1] has sparked renewed attention to the intermediate state (IS) in type-I superconductors [2–6], a classical example of such systems with very rich physics [7]. Besides the equilibrium magnetic flux pattern, unsolved fundamental problems of the IS include the flux density B in the normal (N) domains and the critical field H_{ci} for the IS-N transition. The IS provides access to one of the most fundamental parameters, namely the Pippard/BCS coherence length ξ_0 (the size of Cooper pairs). However, a verified recipe to extract ξ_0 from the IS properties is missing. On the other hand, some properties of the IS, e.g., the field distribution near the sample surface, can be similar to the properties of the mixed state (MS) in type-II superconductors. Therefore, better understanding of the IS can provide new insights in understanding of the MS.

Ever since Landau introduced a laminar model (LLM) for a slab in a perpendicular field [8], many models of the IS have been proposed. However, *none* is fully adequate [9]. In this Rapid Communication we report on an experimental study of the IS performed with a high-purity indium sample and introduce a *comprehensive* theoretical model for a slab in a tilted field. Our model is surprisingly simple. Nevertheless, it allows for *quantitative* evaluation of the IS parameters, including ξ_0 , and sheds new light on fundamental properties of superconductors.

When a type-I superconductor with demagnetizing factor η is subjected to a weak magnetic field H , the sample is in the Meissner state until H reaches $H_i = (1 - \eta)H_c$, H_c being the thermodynamic critical field [7]. At H_i the sample undergoes a transition to the IS, where it breaks up into N and superconducting (S) domains with flux densities B and zero, respectively. Under increasing H the normal fraction $\rho_n = V_n/V$ (where V_n and V are the volumes of N domains and of the sample, respectively) increases until the entire sample becomes normal at H_{ci} . In agreement with the standard paradigm stating that the N phase is unstable at $B < H_c$ [10,11], H_{ci} is assumed equal to [8] or slightly less

than [7,12] H_c . Below we show that this is true only for very thick samples.

The domain shape depends on many factors [13]. An important role is played by purity. Structural and chemical flaws reduce the electron mean free path, hence increasing the Ginzburg-Landau (GL) parameter κ and, therefore, decrease the S/N interface tension γ , the latter being the “driving force” in reaching the ground state. In addition, the flaws create pinning centers, hence reducing domains’ mobility. Therefore, samples for studies of equilibrium flux patterns have to be pure and possess maximum possible γ (minimum κ) [14]. The equilibrium flux pattern is well established for a cylinder in a perpendicular field and a slab in a strongly tilted field [15]. For the latter $\eta = 1$ ($H_i = 0$) and domains are ordered laminae. The IS in the slab can be investigated using magneto-optics (MO) [13]. This is the experiment we performed.

We focus on the following questions. (1) How does the flux density B and the critical field H_{ci} depend on the material parameters, and how do these quantities evolve with magnitude and orientation of H ? (2) How can the domain-wall parameter δ [and therefore the GL $\xi(T)$ and the Pippard ξ_0 coherence lengths] be inferred from the IS structure? The relationship between $\delta(T)$, characterizing the width of the transition region between N and S domains, $\xi(T)$, and ξ_0 depends on the material and its purity. For the pure-limit Pippard superconductors ($\kappa \ll 1$) $\delta(T) = 1.89\xi(T) = 1.4\xi_0/(1 - t)^{0.5}$, where $t = T/T_c$ [7].

At first sight the answers are known [7,11,12,15]. However, ξ_0 in Sn and In, determined from the measurements in the Meissner state (310 nm in Sn and 380 nm in In) [16], differ from ξ_0 calculated from $\delta(0)$ obtained in the IS (180 [17] and 240 nm [18], respectively). Since in both cases the samples were very pure, this signals the inadequacy of models used either in Ref. [16] or in Refs. [17,18]. Resolving this contradiction was the original motivation for this work.

The IS structure was first treated by Landau in 1937 [8]. He established the concept of the surface tension γ (δ was later defined as $8\pi\gamma/H_c^2$ [19]) and proposed the LLM. Assuming that $B = H_c$, Landau calculated the shape of rounded corners

of a cross section of the S laminae. The rounded corners yield an excess energy of the system competing with the interface energy. Minimizing the sum of these energy contributions, Landau obtained the period of the laminar structure, $D = \sqrt{\delta d / f_L(\rho_n)}$, where d is the sample thickness and $f_L(\rho_n)$ is the “spacing function” with $\rho_n = h \equiv H/H_c$; f_L is determined by the shape of the corners [11].

Soon thereafter Landau admitted that the LLM is unstable because roundness of the corners makes B near the surface less than H_c . However, a “branching” model [19], proposed instead of the LLM, was disproved by Meshkovsky and Shalnikov [20]. Owing to that Lifshitz and Sharvin turned back to the LLM and calculated $f_L(\rho_n)$ and B numerically [21]. Identical results were later obtained analytically [22]. In the LLM B , being H_c in the bulk, is $0.66H_c$ near the surface at low H and increases up to H_c at the IS-N transition. Fifty years later direct bulk μ SR measurements of B in a Sn slab in a perpendicular field revealed that $B(H)$ starts from H_c and decreases down to H_{ci} [23]. Such a dependence for $B(H)$ had been anticipated by Tinkham [7].

De Gennes [12] noticed that a positive γ should reduce H_{ci} . Assuming a small reduction, de Gennes obtained for the transverse configuration $H_{ci\perp} = H_c[1 - 0.9(\delta/d)^{0.5}]$.

Tinkham [7] recognized that the dominant contribution to the excess energy term comes from inhomogeneity of the field outside the sample and therefore roundness of the corners can be neglected. Tinkham computed this energy by introducing a “healing length” L_h over which the field relaxes to its uniform state: $L_h^{-1} = D_n^{-1} + D_s^{-1}$, where D_n and D_s are the width of the S and N laminae, respectively. Assuming a rectangular cross section of the laminae and hence a uniform B , allowed to be somewhat less than H_c , Tinkham obtained

$$H_{ci\perp} = H_c[(1 + 4\delta/d)^{0.5} - 2(\delta/d)^{0.5}]. \quad (1)$$

The structure expected from the LLM has *never* been observed. Images reported from the 1950s onward revealed intricate flux patterns, often forming corrugated laminae [13].

Sharvin [17] was the first to observe the ordered laminar pattern in a strongly tilted field for 2-mm-thick Sn [17] and In [18] samples. He measured D at different temperatures and calculated $\delta(T)$ using an extended LLM assuming $B_{\parallel} = H_{\parallel}$ (where B_{\parallel} and H_{\parallel} are in-plane components of B and H , respectively) on top of Landau’s original assumption that $B = H_c$. Sharvin’s equation for D is

$$D^2 = \frac{\delta d}{f_L(\rho_n)} \frac{H_c^2}{H_c^2 - H_{\parallel}^2}. \quad (2)$$

The values of $\delta(0)$ obtained for In and Sn using Eq. (2) [17,18] are those from which we started our story. Faber [14] criticized Eq. (2), arguing that H_{\parallel} can alter the shape of the corners. One may add that if $B_{\parallel} = H_{\parallel}$ the magnetic flux is not conserved and therefore the energy balance in the system must be reconsidered.

From the above it follows that the extended LLM [17] is questionable. Therefore, the values of $\delta(0)$ obtained in Refs. [17,18] are questionable as well. However, the $\delta(T)$ dependence obtained by Sharvin is correct because it agrees with the GL theory (historically, it was in reverse order [7]). Besides, the question of how to extract δ from the IS pattern

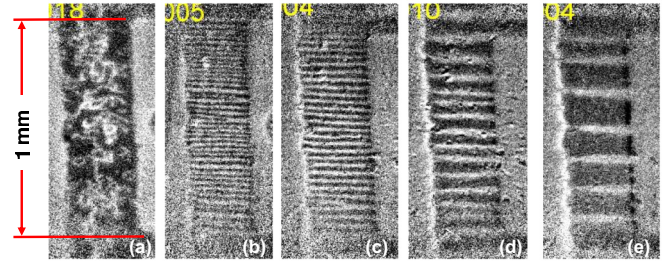


FIG. 1. (Color online) MO images taken at 2.5 K. Superconducting regions are black (H_{\parallel} , H_{\perp} in Oe): (a) (0, 1), (b) (60, 8), (c) (100, 6), (d) (110, 3), (e) (115, 1.3).

in a tilted field remains to be answered. The latter two issues, along with the questions on B and H_{ci} , are addressed below.

The MO imaging was achieved using a setup equipped with a three-dimensional vector magnet [24]. The sample was a 2.5- μ m-thick In film on a SiO₂ wafer. The film residual resistivity ratio was 540. The other film characteristics were the same as those in Ref. [16]. Overall, the film is a Pippard superconductor ($\kappa \simeq 0.07$) in the pure limit. The sample length was 1 mm and the width-to-thickness ratio was 120, implying that for the perpendicular and parallel fields η is 1 and 0, respectively. Images were taken simultaneously with measurements of the electrical resistance R using a small low-frequency (11-Hz) ac.

Typical images are presented in Fig. 1. The flux patterns are laminae independent of the history of the applied field. At $H_{\perp} \lesssim 1$ Oe fractionated laminae were seen in some runs. The laminae are planar and ordered at $H_{\parallel} \gtrsim 0.5H_c$. At smaller H_{\parallel} ($=0.47H_c$ at 1.67 K) slight wavelike corrugations appear. In a perpendicular field the laminae are disordered [Fig. 1(a)]. Therefore, the laminar structure is the ground-state topology of the IS. The same conclusion was drawn by Faber from the experiment with Al ($\kappa \approx 0.01$) sample [14].

While D_n (D_s) increases (decreases) and R varies linearly with H_{\perp} , the period $D = D_n + D_s$, being dependent on H_{\parallel} , is constant for $0.3 \lesssim H_{\perp}/H_{ci\perp} \lesssim 0.8$. Near $H_{\perp} = 0$ and $H_{ci\perp}$ the number of laminae decreases. The IS-N transition for decreasing field is accompanied by deep supercooling of the N state. This confirms the high purity of the sample and verifies that the IS-N transition is a first-order phase transition [15].

Figure 2 presents the sample phase diagram $H_c(T) = H_{c\parallel}(T)$ measured with a dc magnetometer and used for *in situ* temperature determination. It is compared with data measured on other samples and the data from Ref. [25]. The lower curve presents $H_{ci\perp}(T)$ at $H_{\parallel} = 0$, determined from disappearance of the last S lamina in the images and from $R(H_{\perp})$ measurements; the two perfectly coincide. As seen, $H_{ci\perp}(T)$ is *less than half* of $H_c(T)$. The stars represent $H_{ci\perp}$ calculated from Eq. (1) with $\xi_0 = 380$ nm and are clearly consistent with the experimental data. De Gennes’ formula yields $H_{ci\perp}$ considerably exceeding the experimental data. Hence, Tinkham’s interpretation of the excess energy term is used further on.

Since we adopt Tinkham’s approach and, *in agreement with the experimental images*, the N and S domains are assumed to be rectangular parallelepipeds extending in the H_{\parallel} direction. The contribution of the negative surface tension

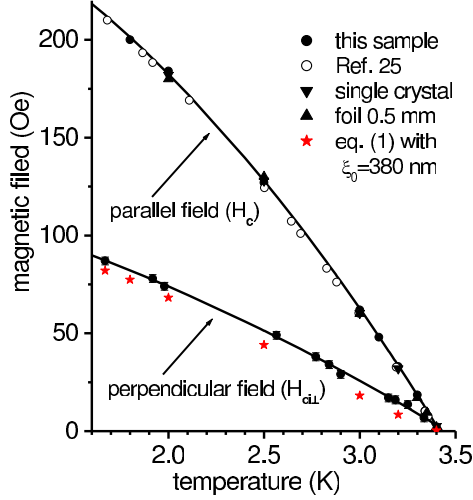


FIG. 2. (Color online) The phase diagram of our sample in parallel and perpendicular fields. The solid curves are parabolic fits of the data obtained with our sample.

at the S/vacuum interface is neglected since the penetration depth is much less than the sample thickness. The out-of-plane and in-plane demagnetizing factors are $\eta_{\perp} = 1$ and $\eta_{\parallel} = 0$, respectively. The former means that $B_{\perp}\rho_n = H_{\perp}$ (conservation of the flux of the out-of-plane component of the magnetic field), whereas the latter means that $B_{\parallel} = H_{\parallel}$ and therefore the flux of B_{\parallel} is not conserved. Hence, the appropriate thermodynamic potential is $\tilde{F} \equiv \tilde{f}V = F - V(B_{\parallel}H_{\parallel}/4\pi) = F - V_n(H_{\parallel}^2/4\pi)$, where F is the free energy and the second term accounts for the work done by the magnet power supply to maintain H_{\parallel} [11]. This term is the *key distinctive element* of our model. We note that this term is neither small (it can exceed the condensation energy) nor trivial (its omission or incorrect form leads to violation of the limiting condition $H_{ci\perp} \rightarrow 0$ at $H_{\parallel} \rightarrow H_c$).

Summing the sample free energy at zero field $V[f_n - H_c^2(1 - \rho_n)/8\pi]$, the energy of the field B in the sample $V\rho_n(B_{\perp}^2 + B_{\parallel}^2)/8\pi$, the energy of the S/N interfaces $2V\gamma/D$, and the excess energy of the field over the healing length $2VL_n(\rho_n B_{\perp}^2 - H_{\perp}^2)/8\pi d$, one obtains

$$\tilde{f} = f_n - (1 - \rho_n)\frac{H_c^2}{8\pi} + \frac{H_{\perp}^2}{8\pi\rho_n} - \rho_n\frac{H_{\parallel}^2}{8\pi} + 2\frac{H_c^2}{8\pi}\frac{\delta}{D} + 2\frac{H_{\perp}^2}{8\pi}\frac{D}{d}(1 - \rho_n)^2, \quad (3)$$

where f_n is the free energy density of the sample in the normal state (magnetic permeability in this state is assumed 1 and therefore f_n does not depend on H).

Similar to the LLM, competition between the last two terms provides the equilibrium D :

$$D^2 = \frac{d\delta}{\rho_n^2(1 - \rho_n)^2} \frac{H_c^2}{B_{\perp}^2} = \frac{d\delta}{(1 - \rho_n)^2} \frac{H_c^2}{H_{\perp}^2}. \quad (4)$$

Substituting Eq. (4) in Eq. (3) and then minimizing $\tilde{f}(\rho_n)$ one obtains the equilibrium ρ_n :

$$\rho_n^2 = h_{\perp}^2/(1 - 4h_{\perp}\sqrt{\delta/d} - h_{\parallel}^2), \quad (5)$$

where $h_{\perp} = H_{\perp}/H_c$ and $h_{\parallel} = H_{\parallel}/H_c$.

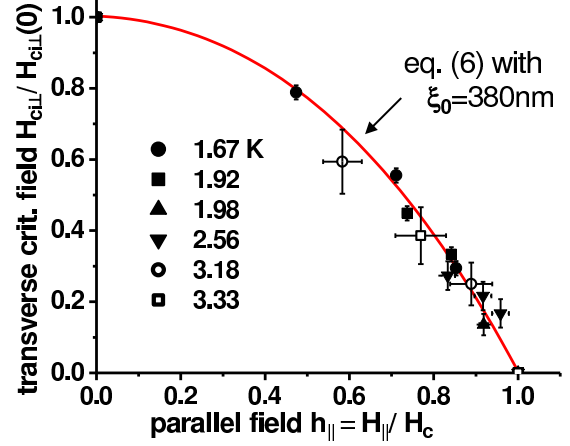


FIG. 3. (Color online) The perpendicular critical field $H_{ci\perp}/H_{ci\perp}(0)$ versus $h_{\parallel} = H_{\parallel}/H_c$. $H_{ci\perp}$ is $H_{ci\perp}$ at $H_{\parallel} = 0$.

At the IS-N transition $\rho_n = 1$, therefore,

$$h_{ci\perp} = \sqrt{4(\delta/d) + 1 - h_{\parallel}^2} - 2\sqrt{\delta/d}. \quad (6)$$

Finally, the reduced flux density $b = B/H_c$ is

$$b^2 = b_{\perp}^2 + b_{\parallel}^2 = h_{\perp}^2/\rho_n^2 + h_{\parallel}^2 = 1 - 4h_{\perp}\sqrt{\delta/d}. \quad (7)$$

The model satisfies the limiting cases, i.e., $\rho_n \rightarrow 0$ at $H_{\perp} \rightarrow 0$ and $H_{ci\perp} \rightarrow 0$ at $H_{\parallel} \rightarrow H_c$. In very thick samples ($\sqrt{\delta/d} \ll 1$) $B = H_c$ and Eq. (4) converts to Eq. (2) if $\rho_n^2(1 - \rho_n)^2$ is replaced by $f_L(\rho_n)$; this explains the correctness of the temperature dependence of $\delta(T)$ in Refs. [17,18].

For a perpendicular field ($H_{\parallel} = 0$) we have that (a) according to Eq. (7) B decreases with increasing H from H_c down to H_{ci} , in agreement with the μ SR results [23] and (b) Eq. (6) reduces to Eq. (1), implying that the theoretical points in Fig. 2 are the same in our model. Hence, our model, developed for a regular laminar structure, can be used for irregular laminar patterns as well.

In Fig. 3 the data for $H_{ci\perp}$ at nonzero H_{\parallel} are compared to the $H_{ci\perp}(H_{\parallel})$ dependence given by Eq. (6). We find that Eq. (6) correctly describes the experimental data.

Figure 4 presents the results for δ at $T = 1.7$ K obtained in three ways. The circles represent δ calculated from Eq. (2) and Eq. (4) using our experimental data for the average D and H_{\perp} at $\rho_n = 0.5$. The dashed line in Fig. 4 represents δ calculated directly using $\xi_0 = 380$ nm. We find that the results following from Eq. (4) agree with the directly calculated value of δ . However, this is not the case for δ obtained using Eq. (2).

Figure 5 presents data for the average D obtained in two runs at $T = 1.7$ K and $H_{\parallel} = 0.85H_c$ and corresponding theoretical curves following from Eqs. (2) and (4). In Eq. (2) D is controlled by f_L ; in our model the spacing function is $f = (1 - \rho_n)^2 h_{\perp}^2$ with ρ_n and h_{\perp} linked by Eq. (5). We find that both f_L and f qualitatively reproduce the experimental data. However, f_L is better at high values of $H_{\perp}/H_{ci\perp}$, whereas f is better at small H_{\perp} . This indicates the importance of the rounded corners at high H_{\perp} , where inhomogeneity of H_{\perp} is minimal.

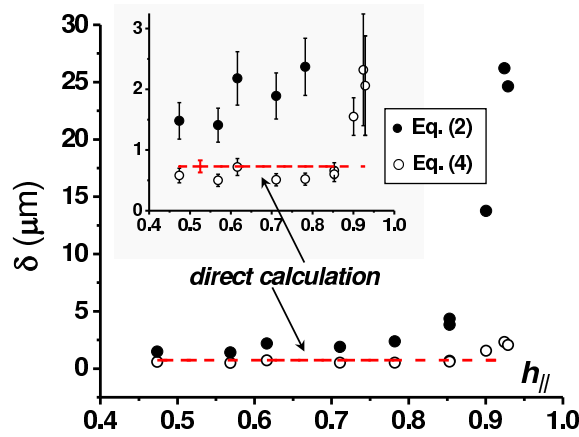


FIG. 4. (Color online) The domain-wall parameter δ inferred from MO images taken at $T = 1.7$ K using Eq. (2) and Eq. (4) plotted on two scales. The dashed line represents the directly calculated $\delta = 1.4\xi_0/(1 - T/T_c)^{0.5}$, $T_c = 3.415$ K, and $\xi_0 = 380$ nm.

In summary, (i) we have performed a magneto-optical study of the IS in a high-purity type-I superconductor resulting in a comprehensive model of the IS for a slab in a tilted magnetic field, which includes the perpendicular field as the limiting case. The model reproduces *all* available experimental data including ξ_0 . Overall, our model is a good first-order approximation of the IS in a slab as advanced by Landau many years ago. (ii) We have shown that a superconducting system in search of the lowest free energy may opt to keep B in the bulk of N domains *considerably* smaller than H_c . This alters the paradigm stating that this is impossible. In type-II materials variation of B in the vortex core can be a factor responsible for the dependence of the core size on the applied field [26]. In that case the core size should also depend on the sample thickness.

We note that the system free energy \tilde{f} [Eq. (3)] (and hence also ρ_n [Eq. (5)], $h_{c\perp}$ [Eq. (6)], and b [Eq. (7)]) depends on δ via the ratio δ/d . Taking into account that δ represents the minimum thickness of the S laminae, the physical significance of δ/d is similar to that of the diameter-to-length

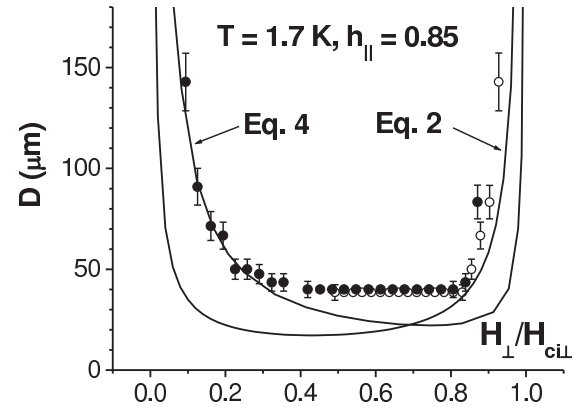


FIG. 5. Experimental data (circles) and theoretical curves for the period of the laminar structure. Solid circles are the data obtained at increasing H_{\perp} with the sample cooled at $H_{\perp} = 0$. Open circles are the data taken after H_{\perp} was reduced from above $H_{c\perp}$ down to $0.5H_{c\perp}$.

ratio of a solenoid where it characterizes the contribution of the inhomogeneous field at the solenoid's ends in the total energy of the magnetic field. For the IS the ratio δ/d characterizes the energy contribution of the inhomogeneous field near the sample surface to the free energy of the system.

A weak point of our model is the oversimplified form of L_h and neglect of the effect of the rounded corners. This is the main reason for the discrepancy between the experimental data and the theoretical curve in Fig. 5 and the deviation of $\rho_n(h_{\perp})$ in Eq. (6) from the linear dependence following from the linearity of $R(H_{\perp})$. To resolve this issue, measurements of the magnetic field near the surface outside and inside the sample are required.

We are grateful for the active interest of Michael E. Fisher and K. A. Kikoin who commented in detail on the manuscript. Discussions with B. Van Schaeuybroeck and correspondence with R. Prozorov are appreciated. This work was supported by NSF (Grant No. DMR 0904157) and by the Research Foundation–Flanders (FWO).

-
- [1] M. Seul and D. Andelman, *Science* **267**, 476 (1995).
 [2] J. Ge, J. Gutierrez, B. Raes, J. Cuppens, and V. V. Moshchalkov, *New J. Phys.* **15**, 033013 (2013).
 [3] G. R. Berdiyrov, A. D. Hernández-Nieves, M. V. Milošević, F. M. Peeters, and D. Domínguez, *Phys. Rev. B* **85**, 092502 (2012).
 [4] M. A. Engbarth, S. J. Bending, and M. V. Milošević, *Phys. Rev. B* **83**, 224504 (2011).
 [5] G. R. Berdiyrov, A. D. Hernández, and F. M. Peeters, *Phys. Rev. Lett.* **103**, 267002 (2009).
 [6] R. Prozorov, A. F. Fidler, J. R. Hobert, and P. C. Canfield, *Nat. Phys.* **4**, 327 (2008).
 [7] M. Tinkham, *Introduction to Superconductivity* (McGraw-Hill, New York, 1996).
 [8] L. D. Landau, *Zh. Eksp. Teor. Fiz.* **7**, 371 (1937) [*Phys. Zs. Sowjet.* **11**, 129 (1937)].
 [9] R. Prozorov, *Phys. Rev. Lett.* **98**, 257001 (2007).
 [10] C. J. Gorter and H. Casimir, *Physica* **1**, 306 (1934).
 [11] L. D. Landau, E. M. Lifshitz, and L. P. Pitaevskii, *Electrodynamics of Continuous Media*, 2nd ed. (Elsevier, Oxford, 1984).
 [12] P. G. de Gennes, *Superconductivity of Metals and Alloys* (Benjamin, New York, 1966).
 [13] R. P. Huebener, *Magnetic Flux Structures in Superconductors*, 2nd ed. (Springer-Verlag, Berlin, 2001).
 [14] I. T. Faber, *Proc. R. Soc. London Ser. A* **248**, 460 (1958).
 [15] A. A. Abrikosov, *Fundamentals of the Theory of Metals* (Elsevier Science, Amsterdam, 1988).
 [16] V. Kozhevnikov, A. Suter, H. Fritzsche, V. Gladilin, A. Volodin, T. Moorkens, M. Trekels, J. Cuppens, B. M. Wojek, T. Prokscha, E. Morenzoni, G. J. Nieuwenhuys, M. J. Van Bael, K. Temst, C. Van Haesendonck, and J. O. Indekeu, *Phys. Rev. B* **87**, 104508 (2013).

- [17] Yu. V. Sharvin, Zh. Eksp. Teor. Fiz. **33**, 1341 (1957) [Sov. Phys. JETP **33**, 1031 (1958)].
- [18] Yu. V. Sharvin, Zh. Eksp. Teor. Fiz. **38**, 298 (1960) [Sov. Phys. JETP **11**, 316 (1960)].
- [19] L. D. Landau, Zh. Eksp. Teor. Fiz. **13**, 377 (1943) [J. Phys. USSR **7**, 99 (1943)].
- [20] A. G. Meshkovsky and A. I. Shalnikov, Zh. Eksp. Teor. Fiz. **17**, 851 (1947).
- [21] E. M. Lifshitz and Yu. V. Sharvin, Dokl. Akad. Nauk SSSR **79**, 783 (1951).
- [22] A. Fortini and E. Paumier, *Phys. Rev. B* **5**, 1850 (1972).
- [23] V. S. Egorov, G. Solt, C. Baines, D. Herlach, and U. Zimmermann, *Phys. Rev. B* **64**, 024524 (2001).
- [24] R. Wijngaarden, C. Aegerter, M. Welling, and K. Heeck, in *Magneto-Optical Imaging*, edited by T. H. Johansen and D. V. Shantsev (Kluwer Academic, Dordrecht, 2003).
- [25] D. K. Finnemore and D. E. Mapother, *Phys. Rev.* **140**, A507 (1965).
- [26] J. E. Sonier, *Rep. Prog. Phys.* **70**, 1717 (2007).